Molecular Crystals and Liquid Crystals Science and Technology. Section A. Molecular Crystals and Liquid Crystals

Publication details, including instructions for authors and subscription information:
http://www.tandfonline.com/loi/gmcl19

Dependence of Resonant SNOM Signal on Various Operation Modes

Jun Ushida [a] & Kikuo Cho [a]

[a] Graduate School of Engineering Science, Osaka University, Toyonaka, 560, Japan

Version of record first published: 04 Oct 2006

To cite this article: Jun Ushida & Kikuo Cho (1998): Dependence of Resonant SNOM Signal on Various Operation Modes, Molecular Crystals and Liquid Crystals Science and Technology. Section A. Molecular Crystals and Liquid Crystals, 314:1, 215-220

To link to this article: http://dx.doi.org/10.1080/10587259808042481

Mol. Cryst. Liq. Cryst., 1998, Vol. 314, pp. 215–220
Reprints available directly from the publisher
Photocopying permitted by license only

Dependence of Resonant SNOM Signal on Various Operation Modes

JUN USHIDA and KIKUO CHO
Graduate School of Engineering Science, Osaka University,
Toyonaka, 560 Japan

A model calculation of resonant Scanning Near-field Optical Microscope (SNOM) by nonlocal response theory is presented with particular attention given to the dependence of the signal intensity on various operation modes. The resonant energies and radiative corrections being independent of the operation mode, the signal difference arises only from the way of extracting information of the resonances in each operation mode. We calculate the signal intensities in irradiation, transmission and reflection modes and characteristic features are demonstrated together with the effect of configuration resonance.

Keyword: resonant SNOM; nonlocal response; irradiation mode; collection mode; reflection mode; configuration resonance

INTRODUCTION

Recently considerable efforts have been devoted to the understanding of the variation of signal intensity in Scanning Near-field Optical Microscope(SNOM)[1]. Though SNOM is commonly accepted as a practical apparatus for surface sensing with high resolution, there are problems in the interpretation of signal intensity. The relevant signal of this microscope is the electromagnetic (EM) field produced by the microscopic polarization induced on a sample. Hence the signal intensity of SNOM contains more information than the topological structure of a sample, especially in a resonant condition, and different features can be extracted by its various operation modes. These operation modes are classified according to the way of sample illumination and signal detection (irradiation, collection and reflection modes) that should be considered in a theoretical

analysis. The purpose of this work is to investigate the dependence of the signal intensity in resonant SNOM on various operation modes based on a microscopic nonlocal response theory.

THEORY

This theoretical framework has been developed in order to properly describe radiation-matter interaction in a confined matter system[2]. This theory allows us to determine the self-consistent motion of matter and radiation field by solving two functional equations:

$$\boldsymbol{A}(\boldsymbol{r},t) = \boldsymbol{A}_0(\boldsymbol{r},t) + \mathcal{G}[\boldsymbol{j}], \tag{1}$$

$$\boldsymbol{j}(\boldsymbol{r},t) = \mathcal{F}[\boldsymbol{A}], \tag{2}$$

where $\boldsymbol{A}$ is vector potential in Coulomb gauge ($\nabla\cdot\boldsymbol{A}=0$), $\boldsymbol{j}$ is current density and $\boldsymbol{A}_0$ stands for the incident light. The nonlocal susceptibility is contained in the functional $\mathcal{F}$ in Eq.(2) as an integral kernel, which is calculated via quantum mechanics of matter system. It has a separable nature as a good approximation for resonant and nonresonant cases[3], and thus the above-mentioned functional equations turn out to be a set of linear equations in the case of linear response. In this manner this scheme can be applied to the various practical calculations of mesoscopic optical responses, where the coherence of matter wave function is well retained[4]-[6].

For the problems of resonant SNOM, it is often convenient to renormalize the effect of substrate into the radiation Green's function, so that the remaining degrees of freedom become small corresponding only to the resonant part of polarization. The outline of this revision is given below and in reference[6], the detailed discussion about it will be given elsewhere.

In terms of polarization $\boldsymbol{P}$ and the transverse part of electric field $\boldsymbol{E}_s$, Eq.(2) takes the following form for linear response

$$\boldsymbol{P}(\boldsymbol{r},\omega) = \sum_{\lambda}\left\{F_{\lambda g}(\omega)\boldsymbol{\rho}_{g\lambda}(\boldsymbol{r}) - F_{g\lambda}(\omega)\boldsymbol{\rho}_{\lambda g}(\boldsymbol{r})\right\}, \tag{3}$$

$$F_{\lambda g} = \frac{1}{E_{\lambda g}-\hbar\omega-i\gamma_\lambda}\frac{E_{\lambda g}}{\hbar\omega}\int d\boldsymbol{r}\,\boldsymbol{\rho}_{\lambda g}(\boldsymbol{r})\cdot\boldsymbol{E}_s(\boldsymbol{r},\omega), \tag{4}$$

where $\gamma_\lambda = +0$, $E_{\lambda g}$ the transition energy from the ground (g) to excited (λ) state, and $\boldsymbol{\rho}_{\lambda g}(\boldsymbol{r})$ the transition dipole density defined as $\boldsymbol{\rho}_{\lambda g}(\boldsymbol{r}) = \langle\lambda|\hat{\boldsymbol{I}}(\boldsymbol{r})|g\rangle\hbar/(iE_{\lambda g})$ in terms of the current density operator $\hat{\boldsymbol{I}}$ in the absent of radiation field. Note that we used the relations, $\boldsymbol{j} = -i\omega\boldsymbol{P}$ and $(i\omega/c)\boldsymbol{A} = \boldsymbol{E}_s$ in ω representation. Eq.(3) and (4) show the separable

nature of the susceptibility. Polarization $\boldsymbol{P}$ can be divided into resonant $\boldsymbol{P}_{\mathrm{r}}$ and nonresonant (background) part $\boldsymbol{P}_{\mathrm{b}}$. Then Maxwell electric field is expressed as follows:

$$\boldsymbol{E}(\boldsymbol{r},\omega) = \boldsymbol{E}_0(\boldsymbol{r},\omega) + \int \mathrm{d}\boldsymbol{r}'\, \overleftrightarrow{\boldsymbol{G}}\,(\boldsymbol{r},\boldsymbol{r}',\omega)\boldsymbol{P}_{\mathrm{r}}(\boldsymbol{r}',\omega), \tag{5}$$

where the background part of the polarization density $\boldsymbol{P}_{\mathrm{b}}$ is renormalized into the radiation Green's function $\overleftrightarrow{\boldsymbol{G}}$. $\boldsymbol{E}_0$ represents the contribution of $\boldsymbol{P}_{\mathrm{b}}$ alone. In this way the simultaneous integral equations, Eq.(3) and Eq.(5), for $\boldsymbol{P}(\boldsymbol{r}), \boldsymbol{E}_{\mathrm{s}}(\boldsymbol{r})$ turn out to be a set of linear algebraic equations for $\{F_{\mu\nu}\}$, which is expressed in a matrix form as

$$\boldsymbol{S}\boldsymbol{F} = \boldsymbol{F}_0, \tag{6}$$

where the column vector $\boldsymbol{F}$ the set of the unknown variables $F_{\mu\nu}$, and $\boldsymbol{F}_0$ contains only the contribution of the field $\boldsymbol{E}_0(\boldsymbol{r},\omega)$. The matrix elements of $\boldsymbol{S}$ contain the retarded interaction via transverse field between two induced dipoles given as

$$\mathcal{R}[\boldsymbol{\rho}_{\mu\nu}, \boldsymbol{\rho}_{\tau\lambda}] = \iint \mathrm{d}\boldsymbol{r}\mathrm{d}\boldsymbol{r}'\, \boldsymbol{\rho}_{\mu\nu}(\boldsymbol{r})\, \overleftrightarrow{\boldsymbol{G}}_{\mathrm{T}}\,(\boldsymbol{r},\boldsymbol{r}',\omega)\boldsymbol{\rho}_{\tau\lambda}(\boldsymbol{r}'), \tag{7}$$

where $\overleftrightarrow{\boldsymbol{G}}_{\mathrm{T}}$ is the transverse part of the dyadic Green's function for EM field. Solving Eq.(6) with the appropriate condition for incident light, we can determine the motion of $\boldsymbol{P}$ and $\boldsymbol{E}_{\mathrm{s}}$ self-consistently.

The dependence on the operation mode arises from [A] how $\boldsymbol{E}(\boldsymbol{r},\omega)$ is detected and [B] how the incident light is sent to the matter, i.e., how the structure of $\boldsymbol{F}_0$ is. The resonances in frequency come from $\boldsymbol{S}^{-1}\boldsymbol{F}_0$. Generally speaking, both $\boldsymbol{S}^{-1}$ and $\boldsymbol{F}_0$ can contain resonances. However, in the model of our present problem $\boldsymbol{F}_0$ arises from the scattering of light from a semi-infinite local dielectric, and therefore, there is no resonance from $\boldsymbol{F}_0$ term. Thus, the resonances are all determined from $\det(\boldsymbol{S}) = 0$. These resonant energies contain the radiative corrections due to Eq.(7), which represent energy shifts and widths. Note that the resonant condition is independent of operation mode. The operation modes determine the (complex) amplitudes with which various resonances are detected,which will be studied in the next section.

MODEL AND NUMERICAL RESULTS

For a model calculation of resonant SNOM we take a model of an assembly of semiconductor spheres for a sample and a probe tip. The radius

of each sphere is $a = 1.5$ nm and the positions of the center of spheres are $(\pm a, 0, 2), (0, \pm\sqrt{3}a, 2)$ for the sample and (x,y,6) for the probe in a Cartesian(x,y,z) coordinate system. A substrate such as a prism supporting the sample is modeled by a semi-infinite local dielectric with $\epsilon_{sub} = 2$, which occupies the half-space $z < 0$. This background contribution can be considered in the framework of the nonlocal response theory by using the renormalized radiation Green's function. Each sphere has resonant level, and the energy of the whole spheres system is determined by the dipole-dipole interaction.

Figure 1 illustrates the definition of various operation modes schematically. Broken (solid) arrows indicate the direction of incident (signal) light. For both irradiation (Fig.1(A)) and reflection mode (Fig.1(B)), the incident light is assumed to irradiate the probe sphere alone. The signal is defined as the intensity of the transmitted field through the boundary of the substrate at a point $(0, 0, -200)$ for irradiation mode, and as the far field intensity produced by the induced polarization on the probe alone for reflection mode. Fig.1(C) exhibits collection mode, in which the signal is collected by the probe tip, so that in the same way as for reflection mode. In this mode the incident light is assumed to be a plane wave in z direction.

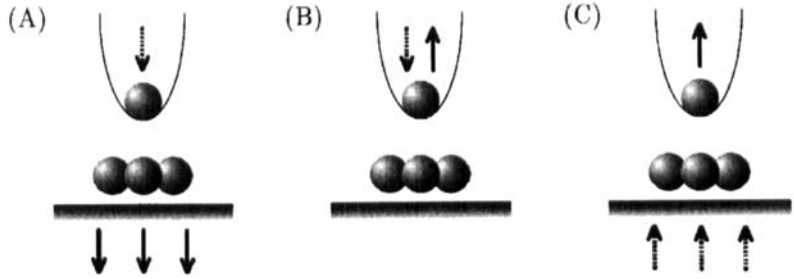

FIGURE 1 Schematic illustration of various operation modes: (A) irradiation mode,(B) reflection mode and (C) collection mode

We executed the numerical calculation in two steps. First, in order to determine the resonant energies we calculated the spectrum with the fixed probe position $(0, \sqrt{3}a, 6)$. A resonant energy consists of matter eigenenergy and a radiative correction including the effect of substrate. A set of these resonant energies is the same for any operation mode. Next the signal intensity in each operation mode was calculated by moving the

probe sphere with a particular resonant energy and the results are shown in Fig.2. The intensity is colored from the minimum intensity (blue) to the maximum (red) linearly. The corresponding resonant energy is noted in the figure caption, which is close to the eigenenergy of the isolated sample spheres. Each figure covers the area $|x| \leq 5$ nm and $|y| \leq 5$ nm.

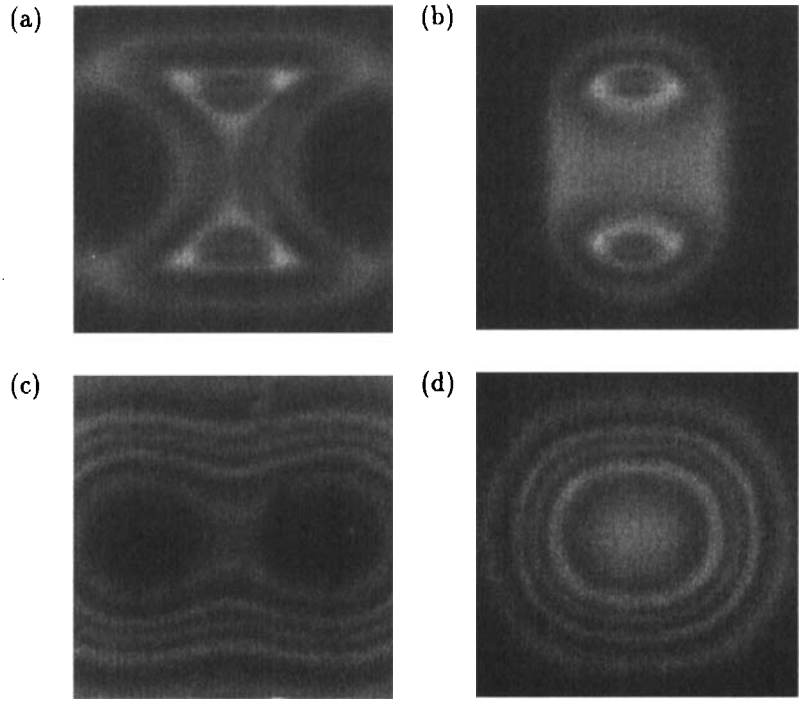

FIGURE 2 Spatial pattern of signal intensity: The resonant energy is 3.2755 eV for (a) and (c), 3.2773 eV for (b) and (d). (a),(b): collection mode, (c),(d): irradiation mode (See Color Plate II).

The difference between Fig.2(a) and 2(b) (or Fig.2(c) and 2(d)) is due to the difference in the eigenmodes of the sample, resonantly excited by different frequency of light. The difference between Fig.2(a) and 2(c) (or Fig.2(b) and 2(d)) is due to the different way of observing the same polarization pattern. The result for reflection mode is very similar to that of collection mode. In collection (or reflection) mode, only the polarization

of the probe sphere contributes to the signal, while in irradiation mode the polarization of all the spheres contributes. Along the red rings of Fig. 2(c) and 2(d), the resonant energy does not change very much, but the amount of polarization on the probe sphere decreases rapidly, as the probe position modes away from $(0, \sqrt{3}a, 6)$, where the frequency of observation is determined.

CONCLUDING REMARKS

Characteristic features of the signal intensity in different operation modes were demonstrated including the effect of configuration resonance. As the eigenvalues and radiative corrections of the whole system including probe, sample spheres and substrate are sensitive to the probe position, a remarkable variation of signal intensity is caused also by the resonant condition. In collection (or reflection) mode, it is possible to identify selectively the probe polarization in the particular eigen mode by the polarization of incident light and its resonant frequency. In irradiation mode the sample and probe polarization can contribute to the signal intensity. This feature can be utilize to extract the local spectroscopic information of the microscopic polarization by comparing the signal intensity maps in different operation mode of SNOM.

Acknowledgments

The computation in this work has been done using the facilities of the Supercomputer Center, Institute for Solid State Physics, University of Tokyo. This work was in part supported by a Grant-in-Aid for Scientific Research on Priority Areas 'Near-field Nano-optics' from the Ministry of Education, Science, Sports and Culture of Japan.

References

[1.] A. Michael et al., *Near Field Optics*, (John Wiley & Sons, 1996).
[2.] K. Cho, *Prog. Theor. Phys. Suppl.*, **106**, 225 (1990).
[3.] Y. Ohfuti and K. Cho, *Phys. Rev. B*, **51**, 14379 (1995) ;
[Errata] ibid., *J. Lumines.*, **66/67**, 94 (1996).
[4.] Y. Ohfuti and K. Cho, *Phys. Rev. B*, **52**, 4828 (1995).
[5.] K. Cho et al. , *Jpn. J. Appl. Phys. Suppl.*, **34**, 267 (1994).
[6.] K. Cho and J. Ushida, *Springer Series in Solid-State Sciences*, (Springer-Verlag,1996), **121**, p.193.